RAPID COMMUNICATIONS

PHYSICAL REVIEW B VOLUME 37, NUMBER 16 1 JUNE 1988

Incommensurate superlattice and 90° twist boundaries in the superconducting phase of Bi-Sr-Ca-Cu-O

C. H. Chen, D. J. Werder, S. H. Liou, H. S. Chen, and M. Hong
AT&T Bell Laboratories, Murray Hill, New Jersey 07974
(Received 4 March 1988)

We have observed an incommensurate superlattice structure in the Bi-Sr-Ca-Cu-O system using electron diffraction. The wave vector of the superlattice, $q=(0,\frac{1}{4.7},1)$, has an incommensurate component along the b axis and a commensurate component along the c axis. Twist boundaries perpendicular to the c axis, across which the crystallographic a and b axes are rotated 90°, are commonly observed in this system.

Bulk superconductivity in cuprate superconductors containing bismuth has now been established through a series of reports by a number of workers.[1-5] One very interesting feature in the structure of this new superconductor is the presence of an incommensurate superlattice structure. The superlattice was determined by x-ray diffraction[4] to be incommensurate along b axis with a periodicity 4.76 times the lattice parameter along b. The sublattice structure was also determined[4] to be orthorhombic (space group *Fmmm*) with cell dimensions of 5.414×5.418 ×30.89 Å. In this paper, we report on the electron-diffraction and high-resolution lattice-image studies of the incommensurate phase. We show that the superlattice modulation wave vector, in addition to the incommensurate component along b, has a commensurate component along c. Furthermore, we have found that the orthorhombic superconducting phase of Bi-Sr-Ca-Cu-O is characterized by the presence of 90° twist boundaries perpendicular to the c axis.

Bulk samples with nominal ratios of Bi-Sr-Ca-Cu of 1:1:1:2 and 2.2:2:0.8:2 were prepared by oxidizing alloys of the four elements with the appropriate ratio. The 1:1:1:2 and 2.2:2:0.8:2 samples exhibit a $T_c(R=0)$ of 79 and 82 K, and diamagnetic signals of 27 and 65%, respectively. Thin samples for transmission electron microscopy were obtained by standard techniques—i.e., mechanical polishing followed by ion milling.

Examination of both samples in the electron microscope shows that both have a mixture of different phases. The phase that was identified by x-ray diffraction as the superconducting phase is found to be a minority phase in the 1:1:1:2 sample and one of the majority phases in the 2.2:2:0.8:2 sample. We did not observe any difference in these two samples as far as the structure of the superconducting phase is concerned. In Fig. 1, we show three selected area electron diffraction patterns with zone axes identified as [100], [1$\bar{1}$0], and [010]. They are related through rotation of the sample with respect to the c axis. Specifically, Figs. 1(b) and 1(c) can be obtained from Fig. 1(a) with 45° and 90° tilts, respectively, with the c axis as the tilting axis. The presence of the incommensurate superlattice is best shown in Fig. 1(a) which represents the b^*-c^* plane of the reciprocal lattice. For clarity, the diffraction pattern of Fig. 1(a) is reproduced and indexed in a schematic pattern shown in Fig. 1(d). The diffraction spots due to multiple reflections are also indicated. The rows of weak diffraction spots as marked by arrows in Fig. 1(c) are also due to multiple reflections since they disappear when the sample is tilted slightly away from the zone axis. We note that a small amount of material with the [100] zone axis parallel to the electron beam [as that shown in Fig. 1(a)] was also included in the area selected to generate the diffraction pattern shown in Fig. 1(c). As a result, very weak incommensurate superlattice reflections are also present in Fig. 1(c). If we disregard the superlattice spots and spots due to multiple reflections, all the diffraction spots in Fig. 1 can be indexed with an

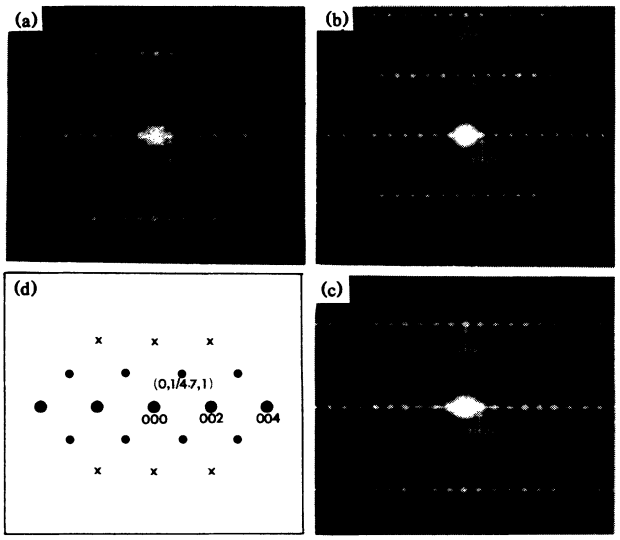

FIG. 1. Electron-diffraction patterns of the (a) [100], (b) [1$\bar{1}$0], and (c) [010], zone axes. (b) and (c) are obtained from (a) with 45° and 90° tilts, respectively, with the c axis as the tilting axis. (d) is a schematic illustration of (a) in which diffraction spots due to sublattice, incommensurate superlattice, and multiple reflections are represented by large dots, small dots, and crosses, respectively.

orthorhombic cell (space groups *Fmmm*) with lattice parameters as determined by the x-ray diffraction.[4] The superlattice modulation wave vector shown in Fig. 1(a) has an incommensurate component along b (~4.7 b) and a commensurate component along c. The superlattice wave vector, therefore, can be written as $Q=G+q$ where $q=(0,\frac{1}{4.7},1)$ is the reduced superlattice wave vector and G is any reciprocal-lattice vector of the sublattice. Our measured incommensurate component along b is in good agreement with that found by x-ray diffraction.[4] However, the c component of superlattice was not reported by the x-ray-diffraction study. The presence of the c component in q gives the difference of superlattice periodicity between the commensurate $(0,\frac{1}{5},1)$ and the incommensurate $(0,\frac{1}{4.76},1)$ phases of ~0.7 Å along the wave-vector direction, whereas the difference would have been as large as 2.3 Å if the c component were not present. The physical origin of the superlattice is not known at the moment, although it has been suggested that formation of superlattice could be due to ordering of Bi—O short bonds[5] or ordering of Sr (or Bi) on the Ca site.[4] With the absence of an a component of the superlattice wave vector, we suspect the superlattice is due to some kind of *rotational* distortion of the Bi—O octahedrons with respect to the a axis. The presence of the c component in the superlattice wave vector requires the Bi—O octahedrons above and below the Ca layer to tilt in opposite directions. From Fig. 1, we also notice the presence of diffuse streaking along the c^* direction. This suggests the existence of lattice disorders or defects in the c direction, which we shall discuss in the next section. No diffuse streakings were observed along a^* or b^* directions.

It is well known that the microstructure of the $YBa_2Cu_3O_7$ superconductor is dominated by the presence of twin domains. The appearance of the twin domains is a way of relieving internal strains that occur in the tetragonal-to-orthorhombic phase transition. In $YBa_2Cu_3O_7$, the twin domains have their c axis in common, with their a and b axes mirrored across the twin boundaries.[6] In the Bi-Sr-Ca-Cu-O superconductor, however, we have observed a new type of phase boundary that can be described as 90° twist phase boundary. These 90° twist boundaries are best illustrated by a high-resolution lattice image shown in Fig. 2. Electron diffraction studies reveal that domains A and B have their c axis in common and are oriented along the [010] and [100] zone axes, respectively. In other words, type-A domains are related to type-B domains by a rotation of 90° with respect to the c axis across the sharp planar boundaries perpendicular to the c axis (marked as TB in Fig. 2). We shall call these kinds of phase boundaries 90° twist boundaries. Figure 2 shows an edge-on view of the 90° boundaries. The microstructure of the Bi-Sr-Ca-Cu-O superconductor is characterized by the presence of these 90° twist boundaries along the c axis, in analogy to the presence of twin boundaries in $YBa_2Cu_3O_7$. We note, however, the 90° twist boundary is different from the twin boundary which requires a mirrored symmetry operation. The 90° twist boundary involves only a rotational symmetry operation across the boundary. We also note that the size of the twist domains could vary from approximately a few hundred to several thousand angstroms.

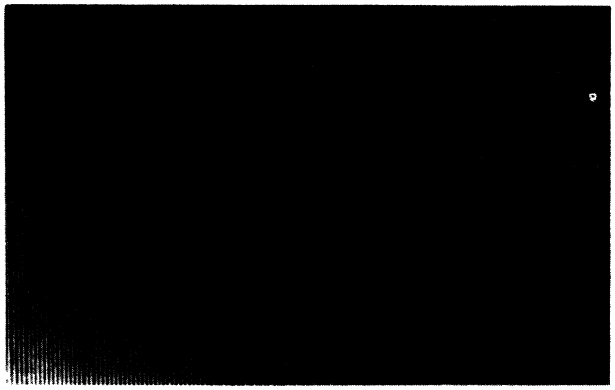

FIG. 2. High-resolution lattice image of 90°-twist domains A and B oriented with zone axis parallel to [010] and [100], respectively. Superlattice fringes are present only in domain B. 90° twist boundaries are marked as TB. Some stacking faults along the c axis are also indicated by arrows.

The 20-Å incommensurate superlattice fringes together with the 31-Å c-axis sublattice fringes are clearly visible in domain B, whereas only the 31-Å c-axis sublattice fringes are seen in domain A. Many stacking faults along the c axis, marked by arrows, can also be seen. We believe that the presence of these stacking faults gives rise to the diffuse streaking observed along the c^* axis. It is very likely that the stacking disorder is due to Bi, Sr, or Ca cations. The 20-Å incommensurate superlattice fringes are not as straight as the c-axis lattice fringes and some waviness of the fringes can be seen, especially at faulty areas. An important question of the incommensurate phase is whether it can be described as a discommensurate phase—i.e., commensurate domains separated by narrow domain walls (or discommensurations). The incommensurate charge-density-wave state in transition-metal dichalocogenides has been known to be discommensurate.[7] Since the lattice images shown in Fig. 2 were taken with a resolution $\lesssim 8$ Å, sharp discommensurations, if any, on the order of lattice parameter along b (~5.4 Å) will not be visible. The high-resolution superlattice image (domain B in Fig. 2) is certainly quite complex and detailed image simulation would be necessary to further our understanding of the incommensurate superlattice in the Bi-Sr-Ca-Cu-O system.

In conclusion, we have carried out electron diffraction studies of the incommensurate superlattice present in the new cuprate superconductors containing bismuth. We found the superlattice can be characterized by a reduced wave vector of $q=(0,\frac{1}{4.7},1)$. The presence of the c component is important in understanding the incommensurate superlattice. The microstructure of this new cuprate superconductor is characterized by the presence of 90° twist-phase boundaries. We also notice that sometimes the superconducting phase is separated by the similar 90° twist boundaries from the semiconducting phase[4] which has a c-axis lattice parameter of 24.5 Å. The fact that the incommensurate superlattice structures are found only in

the b^*-c^* plane and not in the a^*-c^* plane is also consistent with an orthorhombic cell structure and not a tetragonal cell[5] as recently proposed. The high density of stacking faults along the c axis may play an important role in achieving high critical current density.

[1]C. Michel, M. Hervieu, M. M. Borel, A. Grandin, F. Deslandes, J. Provost, and B. Ravean, Z. Phys. B **68**, 421 (1987).

[2]H. Maeda, Y. Tanaka, M. Fukutomi, and T. Asano, Jpn. J. Appl. Phys. Lett. (to be published).

[3]R. M. Hazen, C. T. Prewitt, R. J. Angel, N. L. Ross, L. W. Finger, C. G. Hadidiacos, D. R. Veblen, P. J. Heaney, P. H. Hor, R. L. Meng, Y. Y. Sun, Y. Q. Wang, Y. Y. Xue, Z. J. Huang, L. Gao, J. Bechtold, and C. W. Chu, Phys. Rev. Lett. **60**, 1174 (1988).

[4]S. A. Sunshine, T. Siegrist, L. F. Schneemeyer, D. W. Murphy, R. J. Cava, B. Batlogg, R. B. van Dover, R. M. Fleming, S. H. Glarum, S. Nakahara, R. Farrow, J. J. Krajewski, S. M. Zahurak, J. W. Wasczak, J. H. Marshall, P. Marsh, L. W. Rupp, Jr., and W. F. Peck, Phys. Rev. B (to be published).

[5]J. M. Tarascon, Y. Le Page, P. Barboux, B. G. Bagley, L. H. Greene, W. R. McKinnon, G. W. Hull, M. Giroud, and D. M. Hwang, Phys. Rev. B (to be published).

[6]C. H. Chen, D. J. Werder, S. H. Liou, J. R. Kwo, and M. Hong, Phys. Rev. B **35**, 8767 (1987).

[7]C. H. Chen, J. M. Gibson, and R. M. Fleming, Phys. Rev. B **26**, 184 (1982).

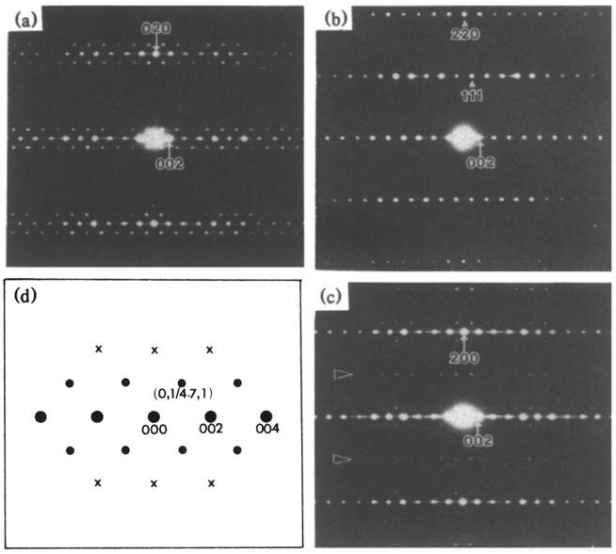

FIG. 1. Electron-diffraction patterns of the (a) [100], (b) [1$\bar{1}$0], and (c) [010], zone axes. (b) and (c) are obtained from (a) with 45° and 90° tilts, respectively, with the *c* axis as the tilting axis. (d) is a schematic illustration of (a) in which diffraction spots due to sublattice, incommensurate superlattice, and multiple reflections are represented by large dots, small dots, and crosses, respectively.

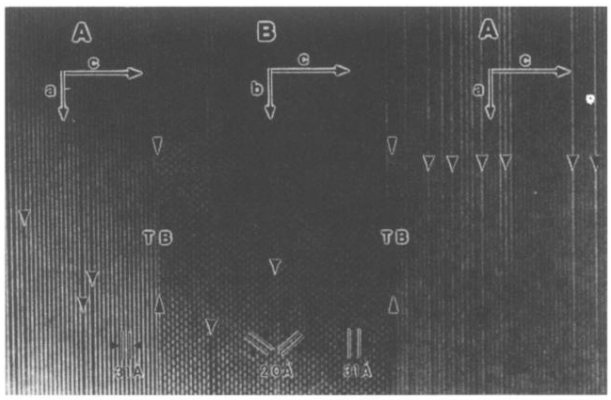

FIG. 2. High-resolution lattice image of 90°-twist domains *A* and *B* oriented with zone axis parallel to [010] and [100], respectively. Superlattice fringes are present only in domain *B*. 90° twist boundaries are marked as TB. Some stacking faults along the *c* axis are also indicated by arrows.